Valence and core excitation spectra in K, Rb, and Cs alkali-metal stage-1 intercalated graphite

L. A. Grunes and J. J. Ritsko*
Xerox Webster Research Center, Building 114, Webster, New York 14580
(Received 6 June 1983)

Excitation spectra of the alkali-metal stage-1 intercalated graphites KC_8, RbC_8, and CsC_8 have been measured by high-resolution (0.1 eV) electron-energy—loss spectroscopy. The π intraband and interband plasmon excitations in the region below 10 eV are the same in all three compounds. However, in the valence region between 15 and 30 eV, small peaks are observed in RbC_8 and CsC_8 which are weaker than those previously observed in KC_8. In KC_8, these structures were identified as both excitations to the backfolded graphite bands created by the introduction of the intercalant and also as characteristic metal-atom core excitations. Within this interpretation, the weakening of the structure due to the backfolded bands with intercalant atomic number is consistent with weakening the coupling far above the Fermi level between the graphite and intercalant atoms. The carbon 1*s* core shell excitation at ~285 eV is also reported. We find that both the spectral shape and threshold energy are unaffected by the choice of alkali-metal intercalant (K, Rb, Cs), although the resulting spectrum differs from that of pristine graphite. Hence the graphite *p* states just above the Fermi level which are probed by the C 1*s* excitation are identically perturbed by the K, Rb, and Cs intercalations, suggesting that the degree of hybridization and charge transfer in these materials is the same.

Intercalation of graphite with alkali metal to stage 1 yields a model layer compound in which the alternating metal and graphite atom planes interact, resulting in a compound exhibiting electronic properties different than those of pristine graphite. In particular, we expect the alkali-metal atoms to at least partially donate their weakly bound outermost *s* electron to the graphite planes. Such charge transfer shifts the Fermi level (E_F) up from its value before intercalation, changing the nature of the highest occupied states. Also, since the alkali-metal valence *s* states are degenerate in energy with the graphite π bands, and since the metal-carbon (*M*-C) interatomic distances are quite small, we may expect to observe hybridization between the metal and the graphite orbitals.

Electron-energy—loss spectroscopy (EELS) has been shown to be a sensitive probe of the electronic properties of intercalated graphite.[1-5] By performing a Kramers-Kronig analysis on the loss data, the real and imaginary parts of the dielectric function may be obtained, and the elementary excitation spectrum of the solid determined. This paper contributes to a growing body of literature and consists of a comparative study at high-energy resolution and statistics of the three alkali-metal graphite intercalated compounds (GIC's) which form an MC_8 stage-1 structure, KC_8, RbC_8, and CsC_8. In the valence portion of the spectrum, we observe features unresolved by previous measurements taken at poorer resolution and statistics.[5] We shall find that those excitations involving states close to the Fermi level are virtually indistinguishable in KC_8 versus RbC_8 versus CsC_8, providing strong evidence that the charge transfer and hybridization of the valence bands in these materials is the same. On the other hand, excitations involving states far from the Fermi level show differences between the three compounds, and we attempt to interpret this unexpected result.

Thin films of KC_8, RbC_8, and CsC_8 were prepared from flakes of graphite (kindly provided by A. Moore of Union Carbide Corporation) with a two-zone vacuum furnace technique described previously.[2] Transmission electron-energy—loss spectra were then recorded for 80-keV incident electrons at zero or finite momentum transfers parallel to the graphite planes with an energy resolution of 0.1 eV full width at half maximum (FWHM) and momentum resolution 0.05 Å^{-1} FWHM.

Figure 1 presents our results for the energy-loss function, $\text{Im}(-1/\epsilon)$, from 0—40 eV at $q=0.1$ Å^{-1} for MC_8, M=K, Rb, Cs. A small correction for multiple inelastic scattering has been applied to the raw measured data.[1]

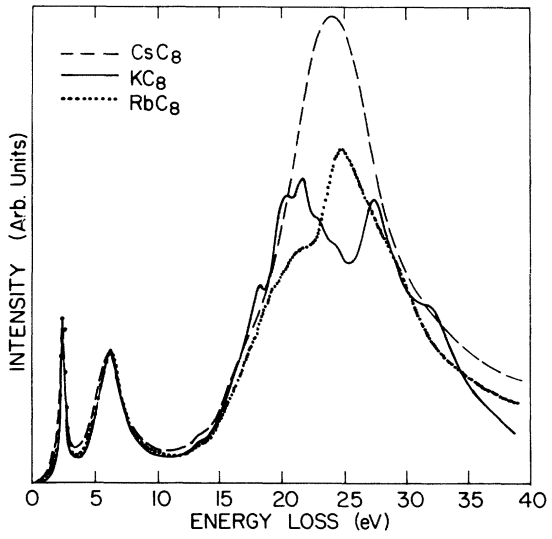

FIG. 1. Electron-energy—loss function from 0 to 40 eV at $q=0.1$ Å^{-1} for KC_8, RbC_8, and CsC_8.

For purpose of comparison, the corrected spectra have also been scaled vertically to match intensities at their peak near 6.2 eV, which is closely related to a similar excitation in pristine graphite (see below). *Absolute* normalization may also be carried out using the oscillator strength sum rule for valence electrons.[1] Using this procedure we find that the $\mathrm{Im}(-1/\epsilon)$ functions in KC_8, RbC_8, and CsC_8 reach maximum values of 1.43, 1.48, and 1.75, respectively. Within the scaling procedures employed in Fig. 1, the low-energy portion of the three spectra are virtually identical. At 2.38, 2.35, and 2.39 (± 0.05) eV in KC_8, RbC_8, and CsC_8, respectively, there is a sharply peaked free-carrier π intraband plasmon associated with the presence of the intercalant.[2] (In pristine graphite, only a weak step at about 1.5 eV is observed.) The interband plasmon at 6.23, 6.25, and 6.19 (± 0.05) eV in KC_8, RbC_8, and CsC_8, respectively, is derived from excitation of graphite π bands similar to those which give rise to the 7-eV interband plasmon in pristine graphite.[1] The intraband and interband plasmons are both associated with $\pi \rightarrow \pi^*$ excitations from states just below to just above the Fermi level. Therefore, the observation that these features appear at nearly identical energies and display nearly identical relative intensities in all three GIC's provides evidence that the graphite band structure in the region of the Fermi level is identically perturbed by all three alkali-metal intercalants.

In contrast to the low-energy portion of the spectra in Fig. 1, in the region above 15 eV we observe gross differences between the three GIC loss functions. Specifically, the main $\pi+\sigma$ valence plasmon observed at 27 eV in pristine graphite[1] is strongly modulated in KC_8, weakly modulated in RbC_8, and not visibly modulated in CsC_8, showing a decreasing trend with increasing intercalant atomic number in the strength of the modulations. In KC_8, the multipeaked structure has been previously decomposed onto atomic K excitations present in the pure

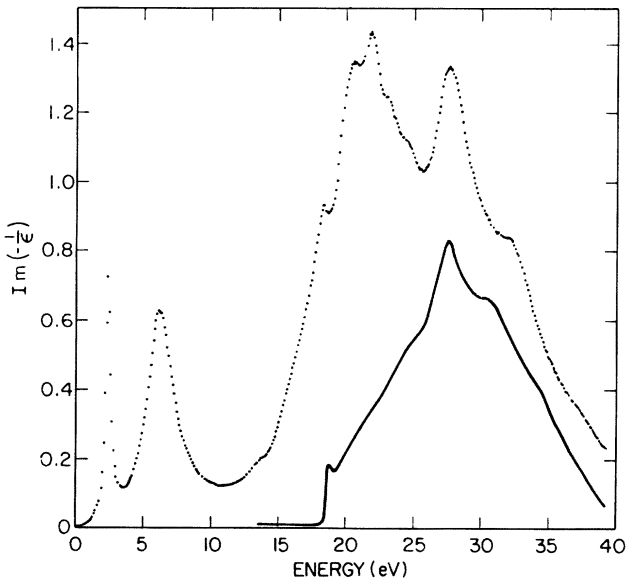

FIG. 2. Electron-energy—loss function for KC_8 compared to K metal $3p$ excitation spectrum (Ref. 6).

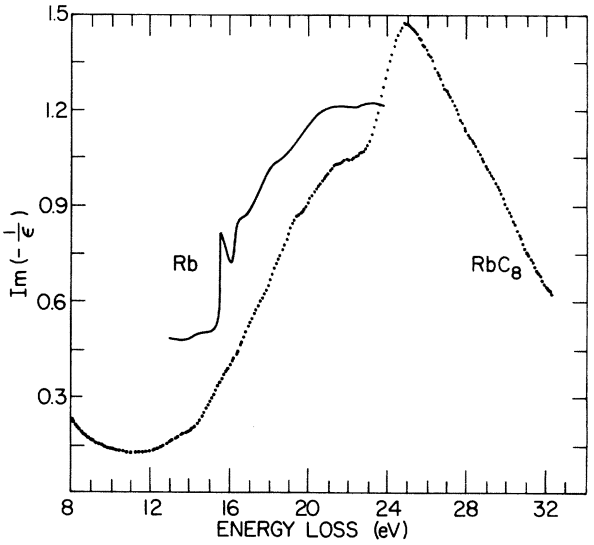

FIG. 3. Electron-energy—loss function for RbC_8 compared to Rb metal $4p$ absorption spectrum (Ref. 7).

metal and into $\pi \rightarrow \pi^*$ graphite backfolded band excitations.[2] Figure 2 (Ref. 2) compares the energy-loss function for KC_8 from Fig. 1 with the K metal $3p$ shell absorption spectrum.[6] Features present in the KC_8 spectrum at 18.4, 27.7, and 32.3 clearly match the K $3p$ spectrum and therefore must arise from atomic excitations of the metal intercalant atoms which are unaffected by the neighboring graphite sheets.

The situation in RbC_8 is less clear-cut. Figure 3 compares our measured energy-loss function for RbC_8 from Fig. 1 with the Rb metal $4p$ absorption spectrum.[7] The close match found between the K and KC_8 features is here absent. Weak features may be discerned in the RbC_8 data at 17.2, 18.4, 19.2, and 21.3 eV showing little obvious correlation in form or energy to the Rb metal peaks at 15.5, 16.5, 18, 21, and 23 eV. For example, there is no sign in RbC_8 of the sharp onset at 15.5 eV in Rb metal, although the corresponding K metal onset is evident in the KC_8 data (Fig. 2). However, the large hump near 21.3 eV in the RbC_8 data does appear to correspond to a similar feature in Rb metal. We conclude that in RbC_8, the Rb metal spectrum must be very weak.

The comparison between the Cs GIC and metal is even less convincing due in part to the decreased strength of the CsC_8 fine structure. Figure 4 shows the CsC_8 energy-loss data from Fig. 1 and the Cs metal $5p$ absorption spectrum.[7] In the region of the Cs metal excitations, the CsC_8 loss function displays no obvious structure. Only very weak maxima appear at 13.3, 15.6, and 17.7 eV, compared to the Cs metal peaks at 12.3, 13.3, 14.0, 15.5, and 18.7 eV. As for RbC_8, no hint of the sharp metal onset is found in the CsC_8 data. The match to the metal peak at 13.3 eV is unimportant, since KC_8, RbC_8, and CsC_8 *all* show a weak hump in their loss functions at ~ 13 eV, while only Cs and not Rb or K metal has absorption structure in this region. Although the 15.6-eV CsC_8 peak seems to match Cs metal, the absence in CsC_8 of any trace of a maximum in the vicinity of the main 18.7-eV Cs metal peak leads us to surmise that the weak structure

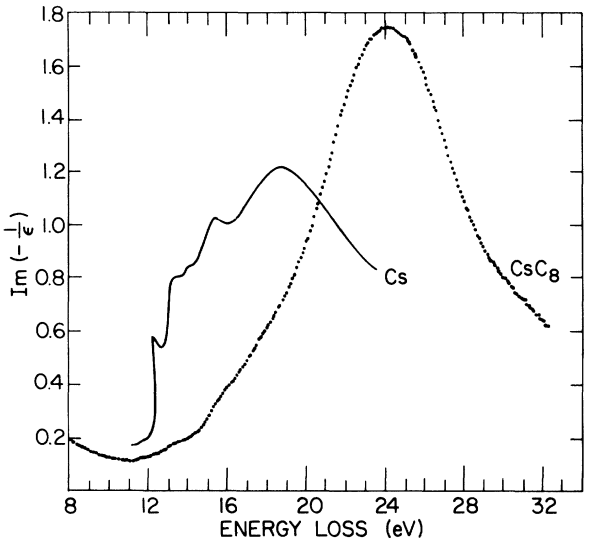

FIG. 4. Electron-energy—loss function for CsC_8 compared to Cs metal $5p$ absorption spectrum (Ref. 7).

displayed by CsC_8 is most likely due to other transitions than atomic Cs excitations.

From our analysis of the spectra shown in Figs. 2—4, we have demonstrated that the match between features in the metal valence absorption and the corresponding GIC loss function degrades from KC_8 to RbC_8 to CsC_8, i.e., as the intercalant atomic number increases. This is a surprising result, since the MC_8 crystal structures of the three GIC's are virtually identical,[8] and since we have shown (Fig. 1) that the low-energy valence intraband and interband plasmons are identical. We see no reason why the metal intercalant should contribute features to the GIC spectrum which are unchanged from the pure metal spectrum in KC_8, but not in RbC_8 or CsC_8. Rather, we hypothesize that the relative cross section for excitations of the intercalant metal p valence shell to excitations of the graphite $\pi+\sigma$ interband transitions must decrease as the intercalant atomic number increases. Hence, compared to KC_8, the metal excitations become less visible in the spectrum of RbC_8, and are virtually washed out in CsC_8. While this explanation is plausible, we know of no fundamental sum rule or other relation which would dictate such a trend.

In order to interpret the remaining nonmetal features in the MC_8 energy-loss functions shown in Figs. 1—4, we consider first the case of KC_8 (Fig. 2). The four loss peaks at 20.6, 21.9, 23.2, and 24.5 eV not identified with K metal have been previously identified by Ritsko and Mele as excitations of the graphite backfolded bands.[2] The metal atoms in the MC_8 GIC structure form a superlattice commensurate with the graphite lattice causing the Brillouin zone to be reduced from that appropriate to graphite. Hence all the graphite zone faces Q are backfolded back into the zone center Γ creating new allowed vertical backfolded band transitions. By considering only the graphite $2p_z$ and $3p_z$ states sticking out from the graphite planes, Ritsko and Mele calculated the strength of the appropriate graphite $\pi\rightarrow\pi^*$ transitions. Since the calculated transitions are related to the imaginary part of the dielectric constant, while the energy-loss function is given by $\mathrm{Im}(-1/\epsilon)=\epsilon_2/(\epsilon_1^2+\epsilon_2^2)$, one must perform a Kramers-Kronig analysis of the energy-loss data to obtain ϵ_1 and ϵ_2 and thereby relate experiment to theory. When Ritsko and Mele perform this analysis on the KC_8 loss data shown in Fig. 1, they obtain an ϵ_2 function which shows three peaks at 21.3, 22.9, and 24.3 eV which, along with a zero crossing of ϵ_1, give rise to the aforementioned four backfolded band peaks in $\mathrm{Im}(-1/\epsilon)$. These three peaks in ϵ_2 are well fit by the backfolded band calculation when reasonable values of the model parameters are chosen. The results of this semiempirical calculation for KC_8 may be extended to RbC_8 and CsC_8 by considering the structural and electronic differences between the three GIC's. In the calculation, the most important parameter is the relative strength of the graphite intraplanar to interplanar interactions. (Metal-atom electronic states are ignored; the only part the metal atoms play is to form a superlattice causing the graphite band backfolding.) Since the interplanar separation increases only slightly with intercalant atomic number, 5.32, 5.65, and 5.95 Å in KC_8, RbC_8, and CsC_8, respectively,[8] no significant change can be expected in the ratio parameter, and hence in the number of calculated backfolded band transitions. We should also consider the neglected effect of varying the strength of the metal-graphite potential however. Owing to the increasing metal ion size, it is likely that the strength of the M^+-graphite interaction potential V_g would decrease with increasing intercalant atomic number. At the GIC reduced Brillouin-zone boundary, the band splitting is proportional to V_g, while the interband transition strength is proportional to V_g^2 (Refs. 2 and 9). Hence, since V_g is weaker in RbC_8 and CsC_8 than in KC_8, we would predict on the basis of the KC_8 calculation that the three backfolded peaks in ϵ_2 found in KC_8 should be weaker and more closely spaced in RbC_8 and CsC_8. Also, because the number of screening electrons surrounding the metal ion core increases with atomic number, the excited electron is more completely screened in CsC_8 versus RbC_8 versus KC_8. Analytically, this would have the effect of reducing the strength of the metal ion pseudopotential which lowers the final-state energy. Therefore, the backfolded band excitations may be expected to decrease in energy from KC_8 to RbC_8 to CsC_8.

The above predictions are consistent with the present experiments, within the limitations of the decreasing visibility of the peaks in RbC_8 and CsC_8. Figures 5 and 6 show the real and imaginary parts of the dielectric function above 10 eV resulting from the Kramers-Kronig analysis of the loss functions of RbC_8 and CsC_8 shown in Fig. 1. The corresponding figure for KC_8 has been published previously.[2] In all three GIC's, a broad, strong peak in ϵ_2 is observed at ~ 14 eV due to graphite $\sigma\rightarrow\sigma^*$ interband transitions.[4] Since these transitions involve electronic states confined to the graphite planes, it is not surprising that the shape, height, and energy of the peak in ϵ_2 is relatively insensitive to the choice of alkali-metal intercalant. However, the peaks in the MC_8 GIC's are similar but *not* identical to the corresponding ϵ_2 peak in pristine graphite, suggesting that even the planar σ bands are affected somewhat by intercalation.

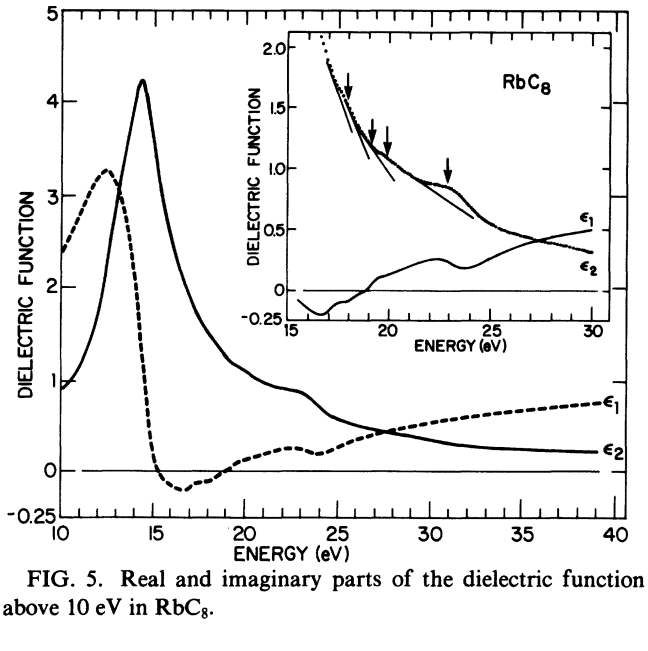

FIG. 5. Real and imaginary parts of the dielectric function above 10 eV in RbC_8.

In addition to the main $\sigma \rightarrow \sigma^*$ interband peak in ϵ_2, secondary maxima in ϵ_2 and corresponding discontinuities in the slope of ϵ_1 are observed in RbC_8 in the inset to Fig. 5 at 17.9, 19.0, 19.9, and 22.8 eV which gives rise to the weak structure observed in the energy-loss function at 17.2, 18.4, 19.2, and 21.3 eV (Fig. 3). In keeping with our identification of the 21.3-eV energy-loss peak as a Rb metal excitation, we also label the maximum in ϵ_2 at 22.8 eV as due to Rb metal. The remaining three weak maxima in RbC_8 are attributed to backfolded band excitations. These features are weaker, more closely spaced, and occur at lower energies than their counterparts in KC_8, consistent with the predicted trends just discussed from the theory of Ritsko *et al.*[2] For CsC_8, no structure is visible on the smoothly decaying tail of the 14-eV $\sigma \rightarrow \sigma^*$ peak in ϵ_2, although the small discontinuities in the slope of ϵ_1 at 16.3 and 18.4 give rise to extremely weak maxima at 15.7 and 17.9 eV in the energy-loss function. It is not possible to connect this observed structure to CsC_8 backfolded band excitations. We surmise that the observed trend of decreased intensity of backfolded band excitations in RbC_8 versus KC_8 is followed through in CsC_8 to the point of invisibility.

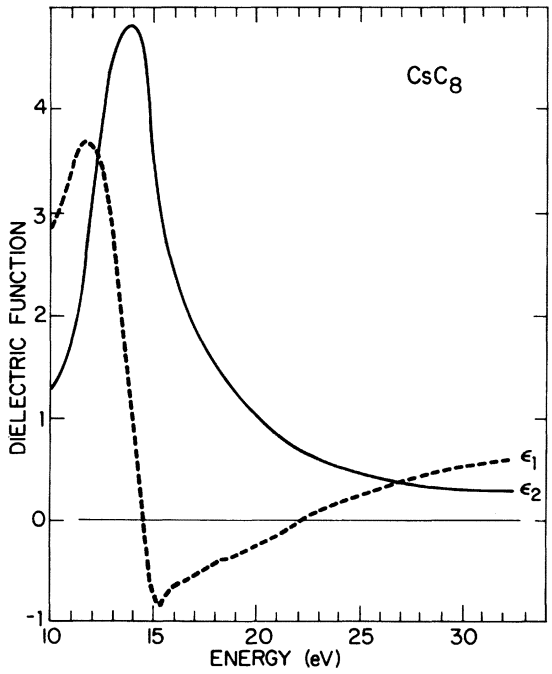

FIG. 6. Real and imaginary parts of the dielectric function above 10 eV in CsC_8.

By comparing the behavior of the ϵ_1 and ϵ_2 functions in the region near the metal p excitations, we may now hypothesize why the metal-derived spectral features get progressively weaker in the GIC energy-loss function from KC_8 to RbC_8 to CsC_8. Peaks will occur in the energy-loss function $\mathrm{Im}(-1/\epsilon)=\epsilon_2/(\epsilon_1^2+\epsilon_2^2)$ near zero crossings of ϵ_1 only if ϵ_2 is small, since when $\epsilon_1 \rightarrow 0$, $\mathrm{Im}(-1/\epsilon) \rightarrow 1/\epsilon_2$. In the MC_8 GIC's considered here, there are 32 C valence electrons for each metal (M) valence electron. Therefore, the dominant feature observed in ϵ_1 and ϵ_2 must be due to C valence excitations. Ignoring M-C hybridization between the respective layers, the MC_8 energy-loss function may be thought of as a superposition of the metal and graphite (including charge transfer electrons) spectra. The metal energy-loss features can contribute noticeably to the combined GIC energy-loss function only in spectral regions where ϵ_1 and ϵ_2 of the C atoms (and therefore of the GIC) are small. In the case of KC_8, the K metal loss peaks at 18.4, 27.7, and 32.3 eV are clearly visible in the KC_8 spectrum and occur far above the dominant C $\sigma \rightarrow \sigma^*$ peak in ϵ_2 near 14 eV, not far from a zero crossing of ϵ_1. For RbC_8 however, the Rb-metal features between 15.5 and 18 eV occur closer on the tail of the large C $\sigma \rightarrow \sigma^*$ peak, where ϵ_2 is not so small. As a result the Rb metal features are barely or not at all discernible in the RbC_8 loss function. However, the wide Rb metal peak centered at ~ 21 eV is further down the C $\sigma \rightarrow \sigma^*$ tail, and hence a corresponding hump *is* observed in the RbC_8 loss function. For CsC_8, the sharp Cs-metal features at ~ 12–16 eV are almost completely washed out of the CsC_8 loss function by their proximity to the 14-eV C $\sigma \rightarrow \sigma^*$ peak in ϵ_2, while the 18.7-eV hump in Cs metal may be too broad to be visible in $\mathrm{Im}(-1/\epsilon)$ due to the rapidly decaying background of ϵ_2. These arguments provide a possible explanation for the disappearance with increasing metal intercalant atomic number of the metal valence excitation from the MC_8 energy-loss functions.

Concluding our discussion of the higher-energy portion of the valence spectra, we note that the observed spectral maxima must be due to transitions involving states far above and/or below the Fermi level. The present results provide evidence that these states must be very different in the three MC_8 GIC's. In particular, we have shown that both the metal-atom–graphite coupling and the relative importance of the metal spectrum decrease rapidly as a function of intercalant atomic number. This is in marked contrast with the states near the Fermi level in these compounds, which give rise to nearly identical energy-loss intraband and interband plasmon spectra.

Figures 7(a) and 7(b) show our results for the real and

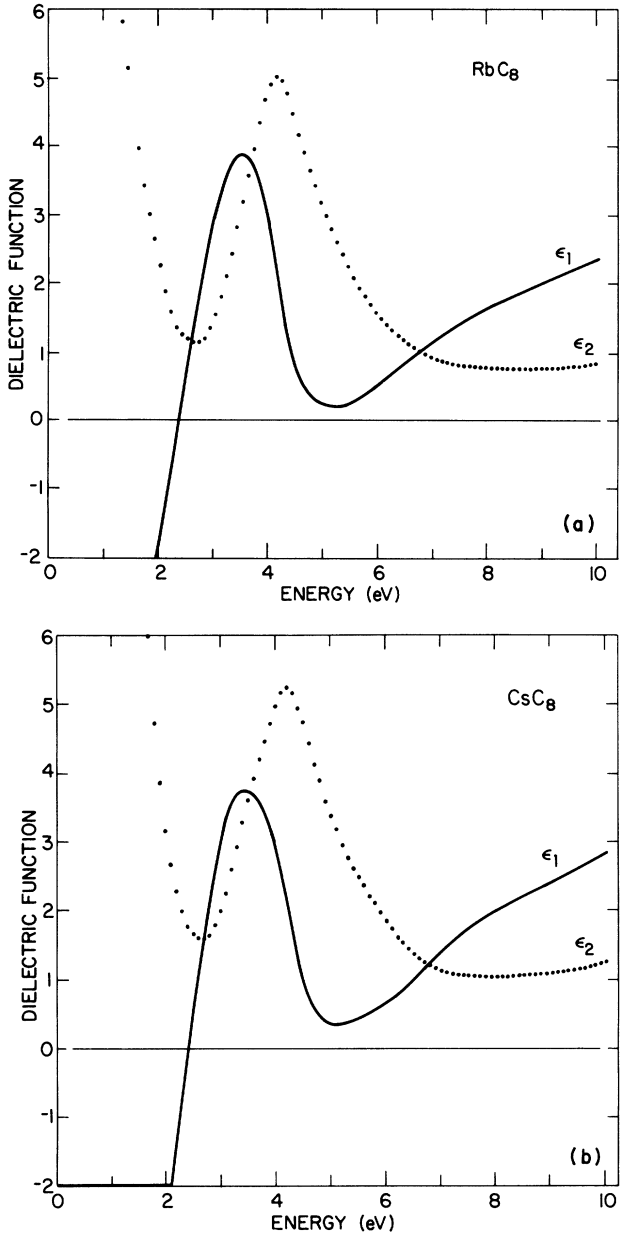

FIG. 7. (a) Real and imaginary parts of the dielectric function below 10 eV in RbC_8. (b) Real and imaginary parts of the dielectric function below 10 eV in CsC_8.

imaginary parts of ϵ of RbC_8 and CsC_8 in the region 0–10 eV. (The corresponding figure for KC_8 has been published previously.[4]) For all three compounds, a zero crossing of ϵ_1 at ~ 2.4 eV produces the sharp intraband plasmon peak in the loss function at the same energy (see Fig. 1), while the broad peak in ϵ_2 centered at 4.0, 4.15, and 4.20 eV in KC_8, RbC_8, and CsC_8, respectively, and the small value of ϵ_1 near 5 eV combine to produce the ~ 6.2-eV interband plasmon energy loss. The ~ 4-eV peak in ϵ_2 is associated with M-point transitions found at 4.3 eV in pristine graphite.[10] DiVincenzo and Rabii[10] have calculated the band structure and density of states (DOS) of KC_8 using a self-consistent Korringa-Kohn-Rostoker (KKR) method, and find that this 4.3-eV M-point transition in pristine graphite is shifted down and split into a series of transitions centered at about 4.1 eV and extending to ± 1.4 eV, in good agreement with the present ϵ_2 data. Using graphical methods previously applied to $C_{6.6}FeCl_3$,[1] we can estimate the threshold for interband transitions from the onset of the M-point peak in ϵ_2. We then correct for the dispersion of the graphite energy bands with q, and obtain an estimate for the interband threshold at $q=0$. Because the π and π^* bands are symmetric with respect to the Fermi level in pristine graphite, the Fermi-level shift upon intercalation is simply half the interband threshold at $q=0$.[11] Using this method, we find that the Fermi level is shifted upward by $\Delta E_F = 1.35$, 1.52, and 1.45 (± 0.15) eV in KC_8, RbC_8, and CsC_8, respectively. Therefore, there is no significant difference within our error limits. Since the charge transfer is directly related to the Fermi-level shift, we conclude that this property is also the same in all three GIC's. However, we are unable to determine absolute charge transfer, since the values are strongly dependent on the particular model of the GIC band structure being used.[4]

We may compare our values for ΔE_F with those obtained via measurements of the conduction bandwidth by ultraviolet photoemission spectroscopy (UPS). Depending on the energy of the incident photon beam, values of 1.4, 1.3, and 1.2 eV at $E_0 \leq 6.5$ eV or 1.25, 1.2, and 1.15 eV at $E_0 = 21.2$ eV are obtained for ΔE_F in KC_8, RbC_8, and CsC_8, respectively.[11] Although our present analysis does

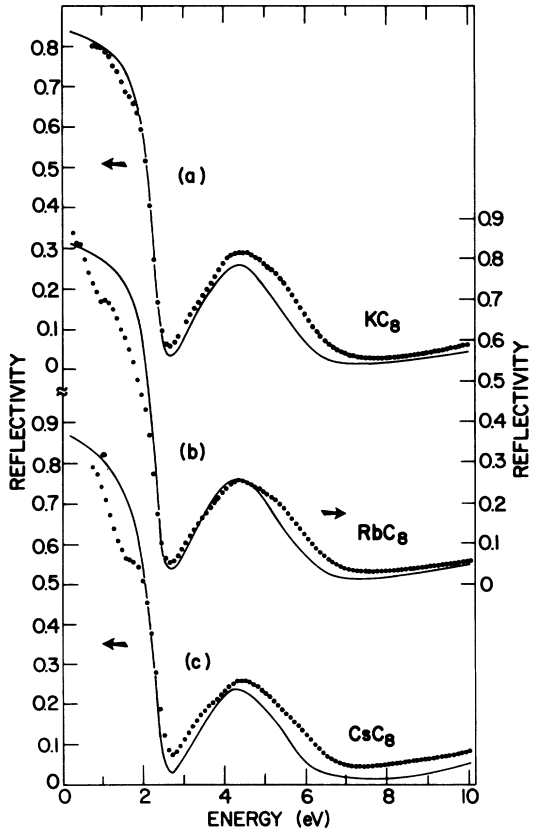

FIG. 8. Normal incidence reflectivity functions. Points are as calculated from present $\mathrm{Im}(-1/\epsilon)$ data. Smooth curves are measured reflectivity of Preil and Fischer (Ref. 12).

not show such a decreasing trend of ΔE_F with intercalant atomic number, it does not contradict it either, since our values are subject to a significant error due to the ambiguities present in our graphical procedure.[1] We do note that our value of $\Delta E_F = 1.35$ eV for KC_8 is identical to the value obtained from the ϵ_2 peak threshold reported by Preil and Fischer[12] from optical reflectivity measurements, and also agrees well with theoretical values of 1.3 and 1.43 eV calculated, respectively, by Inoshita *et al.*[13] and DiVincenzo and Rabii.[10]

The best way to check the validity of the results of a Kramers-Kronig analysis of energy-loss data is to compute the optical reflectivity spectrum from the dielectric function and compare to accurate optical measurements. Figures 8(a), 8(b), and 8(c) show our calculated optical normal incidence reflectivity spectra for KC_8, RbC_8, and CsC_8, respectively, and also the measured optical spectra of Preil and Fischer.[12] Notice that the curves for all three GIC's are essentially identical, in keeping with their nearly identical energy-loss and ϵ_2 functions in this energy region. The match between the two types of data is quite good. Our calculated spectra all show a steep dip at 2.65 eV, reaching a minimum value of 5%, 6.5%, and 8% in KC_8, RbC_8, and CsC_8, respectively. Preil and Fischer's measured data show this dip at the same energy although the minima are somewhat deeper—3.3%, 3.2%, and 3.2% in KC_8, RbC_8, and CsC_8, respectively. The $R(E)$ curves also all show a broad maximum centered at about 4.4 eV, although once again the energy-loss-derived curves are a bit higher than the optical data, e.g., a maximum of 29.5% versus 25.9% for KC_8. Such minor discrepancies may be expected since the energy-loss data were taken at a finite q of 0.1 Å^{-1}, while the optical data correspond to $q=0$. (It is difficult to determine the optical constants or dielectric function from $q=0$ energy-loss data because of the strong energy dependence of the scattering cross section as $q \rightarrow 0$.[1])

Our results for CsC_8 are also in fair agreement with reflectivity data by Pfluger *et al.*[14] which shows the dip to a minimum of $\sim 1\%$ at 2.5 eV, and the broad maximum of $\sim 11.6\%$ centered at ~ 4 eV. Finally, we note that the extra kink present in the energy-loss-derived reflectivity curves at RbC_8 and CsC_8 at ~ 1 and 1.5 eV, respectively, must be due either to an incorrect subtraction of the tail of the zero loss in $\text{Im}(-1/\epsilon)$, or to a residual amount of stage-2 material in our samples. Nonetheless, our calculated prediction of the $R(E)$ function is at least as accurate as the energy-loss functions obtained from a Kramers-Kronig analysis of the optical data.[12]

To complete our analysis of the valence spectra of the MC_8 GIC's, we consider the energy dispersion of the interband plasmon energy loss (Fig. 1) as a function of q, in order to probe the character of the states near the Fermi level. The momentum dependence of a free-electron gas is given by[15]

$$E_p = E_{p0} + \alpha(\hbar^2/m)q^2 ,$$

where m is the free electron mass and E_{p0} is the plasmon energy at $q=0$. For KC_8, Ritsko[4] has reported that the intraband plasmon dispersion was well characterized as free-electron-like for $q > 0.2$ Å^{-1} with $\alpha = 0.8$, and showed

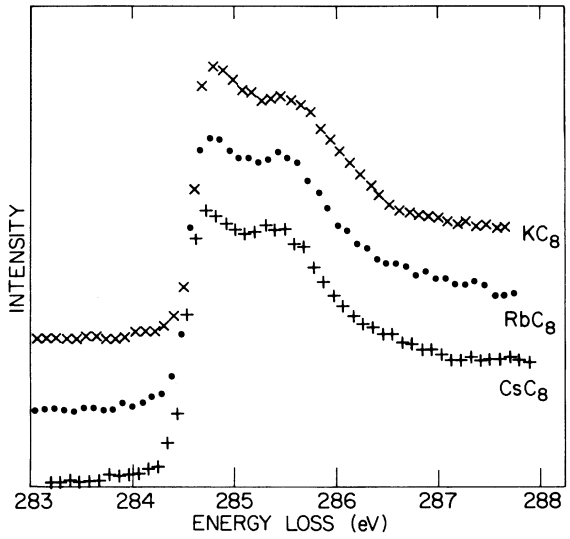

FIG. 9. C 1*s* core excitation spectra for KC_8, RbC_8, and CsC_8.

no dispersion below $q = 0.2$ Å^{-1}. We find the plasmon dispersion in RbC_8 and CsC_8 to be identical to KC_8, providing additional evidence that the states near the Fermi level are the same in all three compounds.

Finally, we consider the C 1*s* core electron-energy—loss spectra measured at $q=0$. In this high-energy region, $\text{Im}(-1/\epsilon) \approx \epsilon_2$, hence the measured core edge structure corresponds directly to electronic C 1*s* transitions into unoccupied states just above E_F. Figure 9 shows our results for KC_8, RbC_8, and CsC_8, in which the spectra are virtually identical; the transitions to the Fermi level are characterized by an extremely sharp rise at threshold followed by two peaks. The threshold and the two following peaks occur at 284.7, 284.9, and 285.6 (± 0.1) eV in KC_8 and at 284.6, 284.8, and 285.5 (± 0.1) eV in RbC_8 and CsC_8. That these features occur at energies within 0.1 eV of each other in all three MC_8 GIC's provides still further evidence that the states just above the Fermi level and also the relative position of the Fermi level to the deeply bound core electrons is independent of the choice of K, Rb, or Cs intercalant.

The double-peaked structure observed in Fig. 9 may be contrasted to the C 1*s* energy-loss spectra in acceptor GIC's.[3] In these materials, the spectra above the pristine graphite Fermi level are identical to graphite, exhibiting only a single narrow peak. Therefore, in acceptor GIC's, the states just above the pristine graphite Fermi level are unperturbed by the introduction of the intercalant. This cannot be the case in the alkali-metal GIC's (AGIC's). Compared to pristine graphite, the AGIC C 1*s* spectra exchibit a steeper rise at threshold plus an additional peak. This second peak is probably a consequence of metal-carbon hybridization, which could cause a splitting of the C $p\pi^*$ graphite bands. However, at present, the band-structure calculations cannot predict our observed double-peaked spectra. For example, in KC_8, semiempirical tight-binding calculations[13] show a DOS above the Fermi level characterized by a peak at E_F associated with the K 4*s* band followed by a second DOS peak at 0.5 eV higher energy due to states closely related to the M point

of pristine graphite. Unfortunately, such a DOS cannot explain our data since C 1*s*→K 4*s* transitions are extremely weak due to negligible overlap of these wave functions. Moreover, the recent analysis of core electron x-ray photoemission spectroscopy (XPS) and EELS experiments by Ritsko and Brucker[16] for KC_8 show that the K 4*s* band minimum lies 2.2 eV *above* the Fermi level. Therefore, the C 1*s* threshold is unrelated to transitions to the K 4*s* band. We also note that since the ionization potentials of KC_8, RbC_8, and CsC_8 decrease with atomic number, the metal valence *s* states are *not* expected to lie at the same energy with respect to the deeply bound C 1*s* state. Therefore, if one of the peaks in our measured spectra were due to 1*s*→*M ns* transitions, the position of that feature would vary between compounds, and this is not observed. Finally, we note that the measured spectra peaks also cannot be related to C 1*s* transitions to the interlayer states present in the band-structure calculations for graphite and KC_8 by Posternak *et al.*[17] again due to negligible overlap of the initial- and final-state wave functions.

As noted above, the KKR band structure for KC_8 of DiVincenzo and Rabii[10] shows the K 4*s* band to be ~1.5 eV above the Fermi level, in good agreement with the determination of Ritsko and Brucker.[16] However, this DOS is not sufficiently accurate to resolve structure in the unoccupied bands which could be related to our observed double-peaked structure. In any case, previous comparisons to theory[3] for acceptor GIC's have shown that it is not possible to directly compare the C 1*s* energy-loss spectrum to the ground-state DOS. This is because the electron-hole interaction strongly influences the spectrum, causing an excitonic enhancement at threshold.[3] Therefore, it may be possible that the abrupt threshold peak observed in the alkali-metal graphite intercalated compound spectra corresponds to an excitonic enhancement effect while the second peak at 0.7 eV higher energy corresponds to transitions to the *M* point states in pristine graphite. However, a definitive explanation of the measured MC_8 C 1*s* spectral features awaits a proper theoretical analysis incorporating both hybridization between the graphite and metal layer wave functions and also the excitonic effects created by the core hole.

Before concluding, we explore the possibility that the double-peaked structure in the three MC_8 C 1*s* spectra might be related to two inequivalent C atom sites in this structure having one or two M^+ nearest neighbors. DiCenzo *et al.*[18] have advanced this type of argument to explain anomalous large widths observed in their XPS spectra of KC_8 and KC_{24}, although they were unable to resolve separate contributions due to the different types of C atoms. Our EELS experiments were conducted at much better energy resolution (0.1 vs ≥0.6 eV) than that obtainable using commerical XPS equipment. Therefore, one might be tempted to claim the double-peaked C 1*s* EELS structure is due to such initial state effects. However, since there are equal numbers of the two inequivalent types of C atoms, one would have to claim that our measured spectra consist of a superposition of two displaced transition peaks with equal intensities. The spectra reported in Fig. 9 are incompatible with such a 1:1 ratio. To illustrate this point, we attempt to construct a model AGIC

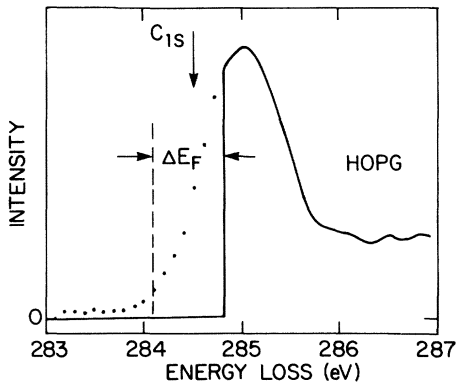

FIG. 10. Construction of hypothetical alkali-metal GIC C 1*s* line shape from pristine graphite spectrum.

spectra by using the C 1*s* edge in (pristine) highly oriented pyrolytic graphite (HOPG—see Fig. 10). In the AGIC, charge transfer from the *M*→C bands causes the Fermi level to shift up by an amount ΔE_F. Since the energy-loss edge measures transitions to states just above E_F, our resulting model AGIC C 1*s* line shape for each type of C site is given by the graphite spectrum for energies above the cutoff energy ($E_F+\Delta E_F$), and by zero below this point. Such a spectral line shape might be expected on the basis of previous measurements of the C 1*s* spectrum in acceptor GIC's.[3] To model the effect of two different C 1*s* binding energies, we simply add two displaced model line shapes together and attempt to fit the AGIC data. The resulting 1:1 HOPG curve shown in Fig. 11 bears no resemblance to the measured KC_8 data. Even at optimized 3:1 superposition the curve fails to fit the data. This is because the rather high cutoff energy needed to model the sharp threshold maximum (Fig. 10) is incompatible with the gently rounded shape of the second-higher energy maximum. Therefore, the line shape of our measured C 1*s* spectra shown in Fig. 9 is unrelated to inequivalent C atoms having different core-level binding energies. Be-

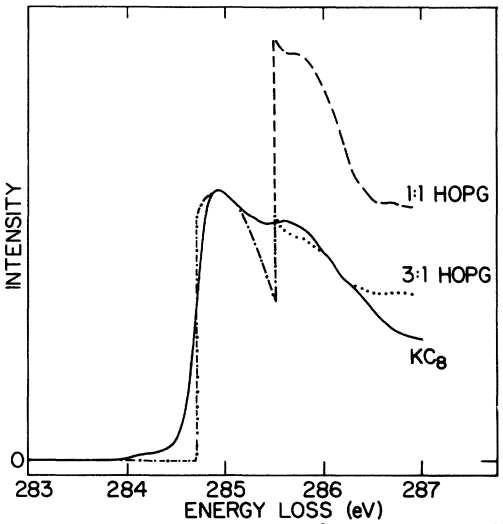

FIG. 11. Unsuccessful comparison of model construction line shapes from two inequivalent C atom sites with measured KC_8 spectrum.

sides, theoretical work in progress by DiVincenzo and Mele[19] indicates that the charge distribution within the graphite planes in the MC_8 AGIC's is close to uniform on the interatomic scale, in contrast with the model of DiCenzo *et al.*[18] We conclude that our double-peaked C 1*s* line shape can only be due to the distribution of C conduction-band states which are influenced by hybridization with the metal wave functions in the presence of the core hole. Since this structure is identical in all three MC_8 AGIC's, the *M*-C hybridization just above the Fermi level must also be the same.

In this paper, we have presented valence- and core-electron excitation spectra in KC_8, RbC_8, and CsC_8 as measured by EELS. In the valence region below 10 eV, the $\pi \rightarrow \pi^*$ intraband and interband excitations show no appreciable difference between compounds. By performing a Kramers-Kronig analysis of the data to determine the ϵ_2 interband threshold, we determine a Fermi-level shift of about 1.4 eV in all three compounds, a value in good agreement with existing experimental and theoretical data. However, in the spectral region between 15 and 30 eV, gross differences are found between compounds. In an attempt to explain the peak origins, we compare other measured GIC spectra with the corresponding metal valence *p* spectra. While the K 3*p* fine structure is unmistakably present in KC_8, the Rb 4*p* fine structure is only weakly evinced in RbC_8, while the search for Cs 5*p* features in CsC_8 appears fruitless. Similarly, the weak excitations previously observed in KC_8 and interpreted as backfolded band excitations become even weaker in RbC_8, and are not discerned in CsC_8. In any case, since excitations in the (15—30)-eV portion of the spectrum necessarily involve states far above and/or below the Fermi level, we must conclude that the *M*-C hybridization of *these* states must be different in all three compounds, in contrast to the states closer to the Fermi level involved in the intraband and interband plasmons.

Finally, the C 1*s* core-level spectra all show the same double-peaked structure which must be due to hybridization of the C $p\pi^*$ and metal valence states just above E_F. That the three MC_8 GIC's all have identical C 1*s* spectra provides corroborating evidence for our interpretation of the $\pi \rightarrow \pi^*$ intraband and interband data, viz., that the graphite states near the Fermi level are identically perturbed by the K, Rb, and Cs intercalants. Hence, the *M*-C hybridization of the states *near* the Fermi level in all three GIC's is the same.

The authors wish to express their thanks to I. P. Gates for sample preparation and experimental assistance, to M. E. Preil and J. E. Fischer for communicating their unpublished reflectivity data, and to D. P. DiVincenzo and E. J. Mele for helpful discussions.

*Present address: IBM Thomas J. Watson Research Center, P.O. Box 218, Yorktown Heights, New York 10598.

[1]J. J. Ritsko and E. J. Mele, Phys. Rev. B 21, 730 (1980).

[2]J. J. Ritsko, E. J. Mele, and I. P. Gates, Phys. Rev. B 24, 6114 (1981); E. J. Mele (private communication).

[3]E. J. Mele and J. J. Ritsko, Phys. Rev. Lett. 43, 68 (1979).

[4]J. J. Ritsko, Phys. Rev. B 25, 6452 (1982).

[5]D. M. Hwang, M. Utlaut, and S. A. Solin, Synth. Met. 3, 81 (1981).

[6]S. E. Schnatterly (unpublished).

[7]T. Tshii, Y. Sakisaka, S. Yamaguchi, T. Hanyu, and H. Ishii, J. Phys. Soc. Jpn. 42, 876 (1977).

[8]S. Y. Leung, M. S. Dresselhaus, C. Underhill, T. Krapchev, G. Dresselhaus, and B. J. Wuensch, Phys. Rev. B 24, 3505 (1981).

[9]N. W. Ashcroft and N. D. Mermin, *Solid State Physics* (Holt, Rinehart and Winston, New York, 1976).

[10]D. P. DiVincenzo and S. Rabii, Phys. Rev. B 25, 4110 (1982).

[11]P. Pfluger and H. J. Güntherodt, in *Festkörperprobleme (Advances in Solid State Physics)*, edited by J. Treusch (Vieweg, Braunschweig, 1981), Vol. 21, p. 271.

[12]M. E. Preil and J. E. Fischer, Solid State Commun. 44, 357 (1982); and private communications.

[13]T. Inoshita, N. Nakao, and H. Kamimura, J. Phys. Soc. Jpn. 43, 1237 (1977); T. Ohno, K. Nakao, and H. Kamimura, *ibid.* 47, 1125 (1979); H. Kamimura, N. Nakao, T. Ohno, and T. Inoshita, Physica 99B, 406 (1980).

[14]P. Pfluger, K. P. Ackermann, R. Lapka, E. Schüpfer, R. Jeker, H. J. Güntherodt, E. Cartier, and F. Heinrich, Synth. Met. 2, 285 (1980).

[15]H. Raether, *Springer Tracts in Modern Physics* (Springer, Berlin, 1965), Vol. 38, p. 85.

[16]J. J. Ritsko and C. F. Brucker, Solid State Commun. 44, 889 (1982).

[17]M. Posternak, A. Baldereschi, A. J. Freeman, E. Wimmer, and M. Weinert, Phys. Rev. Lett. 50, 761 (1983).

[18]S. B. DiCenzo, S. Basu, G. K. Wertheim, D. N. E. Buchanan, and J. E. Fischer, Phys. Rev. B 25, 620 (1982).

[19]D. P. DiVincenzo and E. J. Mele (private communications).